AD-A166 461 THEORETICAL AND EXPERIMENTAL INVESTIGATION OF FLAMESPREADING PROCESSES IN.. (U) ARMY BALLISTIC RESEARCH LAB ABERDEEN PROVING GROUND MD 1/1

UNCLASSIFIED T C MINOR ET AL. FEB 86 RRL-TR-2710 F/G 19/6 NL

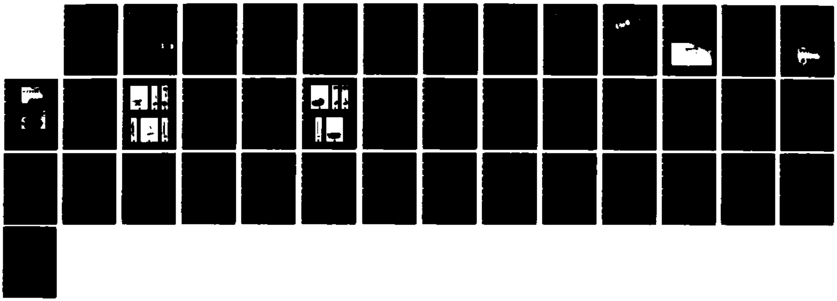

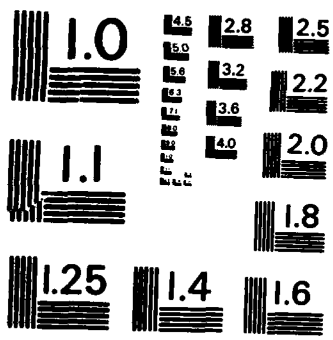

MICROCOPY RESOLUTION TEST CHART
NATIONAL BUREAU OF STANDARDS-1963-A

AD-A166 461

[illegible]

THEORETICAL AND EXPERIMENTAL INVESTIGATION OF FLAMESPREADING PROCESSES IN COMBUSTIBLE-CASED, STICK PROPELLANT CHARGES

[illegible]

[illegible]

February 1986

DTIC
ELECTE
APR 0 7 [illegible]
S D
D

APPROVED FOR PUBLIC RELEASE; DISTRIBUTION UNLIMITED.

US ARMY BALLISTIC RESEARCH LABORATORY
ABERDEEN PROVING GROUND, MARYLAND

DTIC FILE COPY

86 4 7 099

Unclassified

SECURITY CLASSIFICATION OF THIS PAGE (When Data Entered)

REPORT DOCUMENTATION PAGE		READ INSTRUCTIONS BEFORE COMPLETING FORM
1. REPORT NUMBER Technical Report BRL-TR-2710	2. GOVT ACCESSION NO. AD A166 4?1	3. RECIPIENT'S CATALOG NUMBER
4. TITLE (and Subtitle) Theoretical and Experimental Investigation of Flamespreading Processes in Combustible-Cased, Stick Propellant Charges		5. TYPE OF REPORT & PERIOD COVERED Technical Report Jun 84 - Sep 84
		6. PERFORMING ORG. REPORT NUMBER
7. AUTHOR(s) Thomas C. Minor Albert W. Horst		8. CONTRACT OR GRANT NUMBER(s)
9. PERFORMING ORGANIZATION NAME AND ADDRESS Ballistic Research Laboratory SLCBR-IB Aberdeen Proving Ground, MD 21005-5066		10. PROGRAM ELEMENT, PROJECT, TASK AREA & WORK UNIT NUMBERS 1L161102AH43 1L162618AH80
11. CONTROLLING OFFICE NAME AND ADDRESS Ballistic Research Laboratory SLCBR-DD-T Aberdeen Proving Ground, MD 21005-5066		12. REPORT DATE February 1986
		13. NUMBER OF PAGES 39
14. MONITORING AGENCY NAME & ADDRESS (if different from Controlling Office)		15. SECURITY CLASS. (of this report) Unclassified
		15a. DECLASSIFICATION/DOWNGRADING SCHEDULE

16. DISTRIBUTION STATEMENT (of this Report)

Approved for public release; distribution unlimited.

17. DISTRIBUTION STATEMENT (of the abstract entered in Block 20, if different from Report)

18. SUPPLEMENTARY NOTES

Presented in part at 21st JANNAF Combustion Meeting and 8th International Symposium on Ballistics.

19. KEY WORDS (Continue on reverse side if necessary and identify by block number)

Stick Propellants	Interior Ballistics	Ignition
Combustible Case	Interior Ballistic Modeling	NOVA Code
M203E2 Propelling Charge	Multiphase Flow Interior	TDNOVA Code
M203A1 Propelling Charge	Ballistic Modeling	Artillery Charges

20. ABSTRACT (Continue on reverse side if necessary and identify by block number)

Attention has shifted over recent years in the United States to the use of stick propellant in high-performance artillery charges. The substitution of the natural flow channels offered by a bundle of stick propellant over the tortuous path encountered in a bed of granular propellant all but eliminates the problem of pressure waves so often associated with high-pressure gun malfunctions. Further, performance advantages may be realizable because of the higher natural loading density of stick propellant as well as unique hydrodynamic features associated with its geometry. However, recent testing

DD FORM 1473, 1 JAN 73 EDITION OF 1 NOV 65 IS OBSOLETE

Unclassified

SECURITY CLASSIFICATION OF THIS PAGE (When Data Entered)

Abstract (cont.)

has revealed that the postulated flow of igniter gases and flamespreading from the basepad forward through the bundle of sticks in a simple, one-dimensional manner may be significantly complicated by the presence of a combustible case, the initial permeability, mechanical strength, and ignition and combustion characteristics of which may play major roles themselves in characterizing the aforementioned sequence of events.

designated M203E2 and type classified M203A1

The US Army has just completed development of a new top-zone propelling charge to replace the M203 Charge for the 155-mm, M198 Towed Howitzer. The new charge, designated M203E2 during development and type classified M203A1, features M31-type stick propellant and a rigid, combustible cartridge case. A number of these charges were modified to permit direct viewing of the interior of the charge and fired in the Ballistic Research Laboratory 155-mm Howitzer Simulator using transparent plastic chambers. Instrumentation included high-speed cinematography, flash radiography, spindle pressure gages, and projectile base pressure and force transducers. Testing revealed such phenomena as separation and rearward motion of portions of the basepad igniter and rear igniter portion of the case, preferential flow of igniter gases around the outside of the charge, and substantial radial compaction of the charge.

Companion calculations were performed using the TDNOVA two-dimensional, two-phase interior ballistic code. Simulations are presented, for various case configurations, which describe flame propagation, gas flow, and solid-phase motion during the early portion of the interior ballistic cycle. An attempt is made to use these results to aid in the interpretation of experimentally observed behavior.

TABLE OF CONTENTS

LIST OF ILLUSTRATIONS

I. INTRODUCTION

The advantages of stick propellants over granular propellants, especially in high-performance propelling charges, have long been known. The natural channels presented by a bundle of stick propellant offer substantially less resistance to the flow of igniter and early combustion gases, leading to a significant reduction in the potential for the formation of axial pressure waves[1-4] and facilitating the use of simple basepad ignition systems. Moreover, the higher loading density made possible by the regular packing of the stick geometry allows the use of a larger charge weight of a cooler, lower-energy propellant to achieve the same performance, with possible benefits in terms of barrel wear and muzzle flash and blast. (The reduction in barrel wear from the cooler propellant, however, may be at least partially offset by hydrodynamic considerations mentioned below.[5]) Alternatively, the higher loading density may be exploited for increased performance with existing propellant formulations. The stick propellant configuration also helps to provide rigidity to the charge assembly, facilitating handling and loading operations. Finally, a substantial reduction in charge motion during the combustion cycle, a result of the lowered interphase drag, has recently been shown to contribute, via several interesting mechanisms, to an increase in ballistic efficiency for stick propellant charges not predicted by classical interior ballistic models.[6] Several foreign propelling charges currently use stick propellant, notably the Tri-Partite (UK, Germany, Italy) charges for the 155-mm, FH70 Howitzer. Until recently, however, stick propellants have seen little or no application in US charges, primarily due to a lack of a large-scale manufacturing capability. Efforts are now underway to upgrade US propellant manufacturing facilities, and charges employing stick propellant are now under development for both artillery and tank guns. Our research in the

---

[1] S. Weiner, "Investigation of Stick Propellant for 155-mm, XM198," Interim Memorandum Report, Picatinny Arsenal, Dover, NJ, July 1975.

[2] T.C. Smith, "Experimental Gun Testing of High Density Multiperforated Stick Propellant Charge Assemblies," 17th JANNAF Combustion Meeting, CPIA Publication 329, Vol. II, pp. 119-124, November 1980.

[3] F.W. Robbins, J.A. Kudzal, J.A. McWilliams, and P.S. Gough, "Experimental Determination of Stick Charge Flow Resistance," 17th JANNAF Combustion Meeting, CPIA Publication 329, Vol. II, pp. 97-118, November 1983.

[4] T.C. Minor, "Mitigation of Ignition-Induced, Two-Phase Flow Dynamics Through the Use of Stick Propellants," ARBRL-TR-02508, Ballistic Research Laboratory, USA ARRADCOM, Aberdeen Proving Ground, MD, August 1980 (AD A133685).

[5] A.W. Horst, "A Comparison of Barrel-Heating Processes for Granular and Stick Propellant Charges," ARBRL-MR-03193, Ballistic Research Laboratory, USA ARRADCOM, Aberdeen Proving Ground, MD, August 1982 (AD A118394).

[6] F.W. Robbins and A.W. Horst, "Slotted Stick Propellant Study," 20th JANNAF Combustion Meeting, CPIA Publication 383, Vol. I, pp. 377-386, October 1983.

area has been motivated by a need to provide a detailed understanding of the phenomenology of stick propellant charges, both to assist in the performance of development programs and to exploit fully all potential advantages.

We have previously reported on the application of advanced experimental and interior ballistic modeling techniques to the problems of base- and centercore-ignited, granular propelling charges.[7-10] In those studies, our interest centered on the complex interplay between igniter, ullage, and propellant packaging and its influence on the path of flamespreading, the formation of pressure waves, and movement of the solid phase. In the current work with stick charges, we are dealing with a configuration which substantially reduces the problem of pressure waves -- but not without exhibiting some very interesting and yet to be totally understood features of its own.

We begin by looking at a schematic representation of the early portion of the interior ballistic cycle for a stick propellant charge configured for an artillery application (Figure 1). Functioning involves initiation of the basepad by a primer and subsequent transfer of ignition to the stick propellant itself. The igniter gases are expected to penetrate easily through the bundle of sticks, with flamespread proceeding rapidly in a one-dimensional fashion. Some portion of the igniter gases may be expected to flow around rather than through the charge, but to a lesser degree than might be expected with a granular charge. There does exist some photographic evidence that such a charge may ignite nearly uniformly over its entire length after being bathed for a sufficient time in hot igniter gases.[10] However, the flow of igniter gases and the path of flamespreading <u>within</u> the long perforations of stick propellant, particularly if unslotted, are largely unknown and must be assumed to proceed independently of corresponding processes in the interstices. Nevertheless, the minimal resistance to axial flow and the accompanying near uniformity of pressurization over the length of the charge, at least in the

---

[7]A.W. Horst and T.C. Minor, "Ignition-Induced Flow Dynamics in Bagged-Charge Artillery," ARBRL-TR-02257, Ballistic Research Laboratory, USA ARRADCOM, Aberdeen Proving Ground, MD, August 1980 (AD A090681).

[8]A.W. Horst and P.S. Gough, "Modeling Ignition and Flamespread Phenomena in Bagged Artillery Charges," ARBRL-TR-02263, Ballistic Research Laboratory, USA ARRADCOM, Aberdeen Proving Ground, MD, September 1980 (AD A091790).

[9]A.W. Horst, F.W. Robbins, and P.S. Gough, "A Two-Dimensional, Two-Phase Flow Simulation of Ignition, Flamespread, and Pressure-Wave Phenomena in the 155-mm Howitzer," ARBRL-TR-02414, Ballistic Research Laboratory, USA ARRADCOM, Aberdeen Proving Ground, MD, July 1982 (AD A119148).

[10]T.C. Minor, "Experimental Studies of Multidimensional Two-Phase Flow Processes in Interior Ballistics," ARBRL-MR-03248, Ballistic Research Laboratory, USA ARRADCOM, Aberdeen Proving Ground, MD, April 1983 (AD A128034).

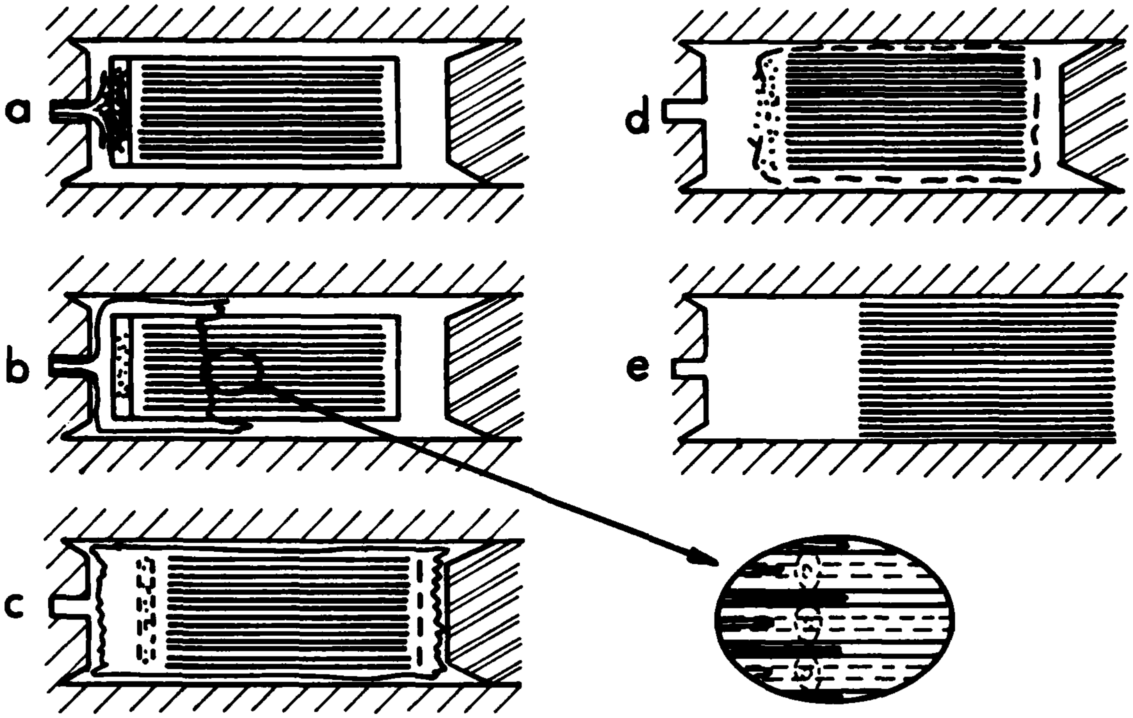

Figure 1. Stick Propelling Charge Phenomenology

interstices, are apparently responsible for the observed substantial reduction in both charge motion and pressure waves which accompany the stick propellant configuration.[10,11]

Several other features need be mentioned before concluding our background remarks on stick charge phenomenology. The first relates to the mechanical behavior of the stick propellant in the ignition environment. Once ignition does occur within the long perforations, rapid internal pressurization in excess of that in the interstices could lead to splitting or fracture of the sticks, yielding an unprogrammed burning surface. Slotted configurations may well reduce the pressure differential between inner and outer regions but may also substantially weaken the sticks. Further, the ability of stick propellant to support reasonable tensile loads without being broken and carried downbore by interphase drag forces (as is granular propellant) is expected to result in most of the propellant charge being burned within the gun chamber itself and should be expected, as mentioned earlier, to impact on both gun performance and tube life. Finally, we must recognize that the above processes are all potentially complicated by the presence of a propellant charge case, the initial impermeability, mechanical strength, and ignition and combustion characteristics of which may play major roles themselves in the above sequence of events.

---

[11]T.C. Minor and A.W. Horst, "Ignition Phenomena in Developmental, Stick-Propellant, Combustible-Cased, 155-mm, M203E2 Propelling Charges," ARBRL-TR-02568, Ballistic Research Laboratory, ARDC, USA AMCCOM, Aberdeen Proving Ground, MD, July 1984 (AD A145283).

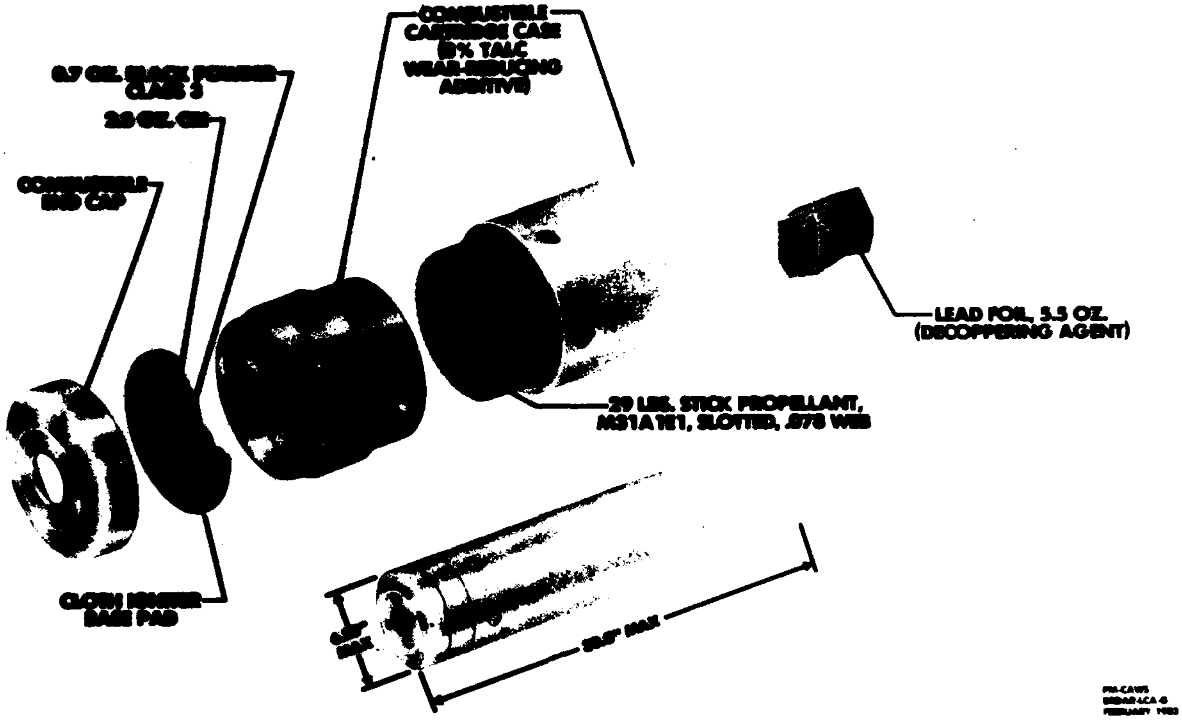

Figure 2. 155-mm, M203E2 Propelling Charge

Studies reported herein all address the 155-mm, M203E2 Propelling Charge, undergoing development at the time of this study by the Large Caliber Weapon Systems Laboratory (LCWSL) of the Armament Research and Development Center at Dover, NJ, for the 155-mm, M198 Howitzer. This charge, pictured in Figure 2, employs an M31-type, triple-base stick propellant in a slotted, single-perforated configuration. The propellant is packaged in a rigid, combustible case, and is ignited by a basepad containing a main charge of Clean Burning Igniter (CBI) and a smaller quantity of Class 3 black powder. Our attention was initially directed to this configuration because of an early, limited test using experimental propellant which yielded higher maximum pressures at cold temperatures than at ambient or hot temperatures. Subsequently, our research has grown to include the experimental and theoretical investigation of the detailed phenomenology of stick propellant charges in general, focusing on the roles of flamespreading, case ignition and rupture, propellant motion and possible fracture, and mechanisms for enhanced burning within long perforations as potential sources of any such anomalous performance.

II. EXPERIMENTAL TECHNIQUES

The vehicle used for the firing tests in this study was the M203E2 Propelling Charge, identical to that illustrated in Figure 2 with the exception of the base igniter. These tests employed the most current igniter design, a doughnut configuration with a central spot of 19.85 g of Class 3 black powder surrounded by an annulus of 28.35 g of CBI. The experimental aspects of this program primarily focused on the impediments to flow of igniter gases into the propellant bed. Accordingly, the two configurations tested in this study were identical, except that one of them had the perforated wall separating the igniter from the stick propellant bed removed.

For completeness, we reference similar, earlier tests[11] performed on candidate M203E2 Propelling Charges in which there was an additional, impermeable boundary, namely a sheet of cellulose nitrate, between the igniter and the propellant bed. In one test with the barrier in place, it was noted that the igniter products did not permeate the stick propellant bed, but rather took the path of less resistance and filled the radial ullage surrounding the charge. In this instance, with the gases pressurizing the chamber outside the charge more than inside the combustible case, the charge was seen to suffer severe radial compaction. In a companion experiment in which this plastic barrier was removed, the igniter gases were seen to enter the charge much more easily, and indeed, the case was seen to rupture from the internal pressurization.

A. Apparatus

Figure 3 depicts the apparatus used at the Ballistic Research Laboratory to conduct the experimental investigation. The illustration shows the mount with a clear plastic simulator for the 155-mm chamber in place. Although the mount also accepts higher-pressure, filament-wound fiberglass chambers, the plastic chambers were used in this study to permit better view of the events transpiring within. The muzzle end of the chamber was closed by a projectile seated in a section of gun tube machined to the dimensions of the M199 Cannon. The breech end of the chamber was closed by a spindle similar to the mushroom configuration of the M185 Cannon with the centrally venting primer spithole, housing three piezoelectric pressure transducers. An instrumented baseplate (Figure 4) was attached to the base of the projectile; it permitted two gas pressure, three total force, and two acceleration measurements at the projectile base.

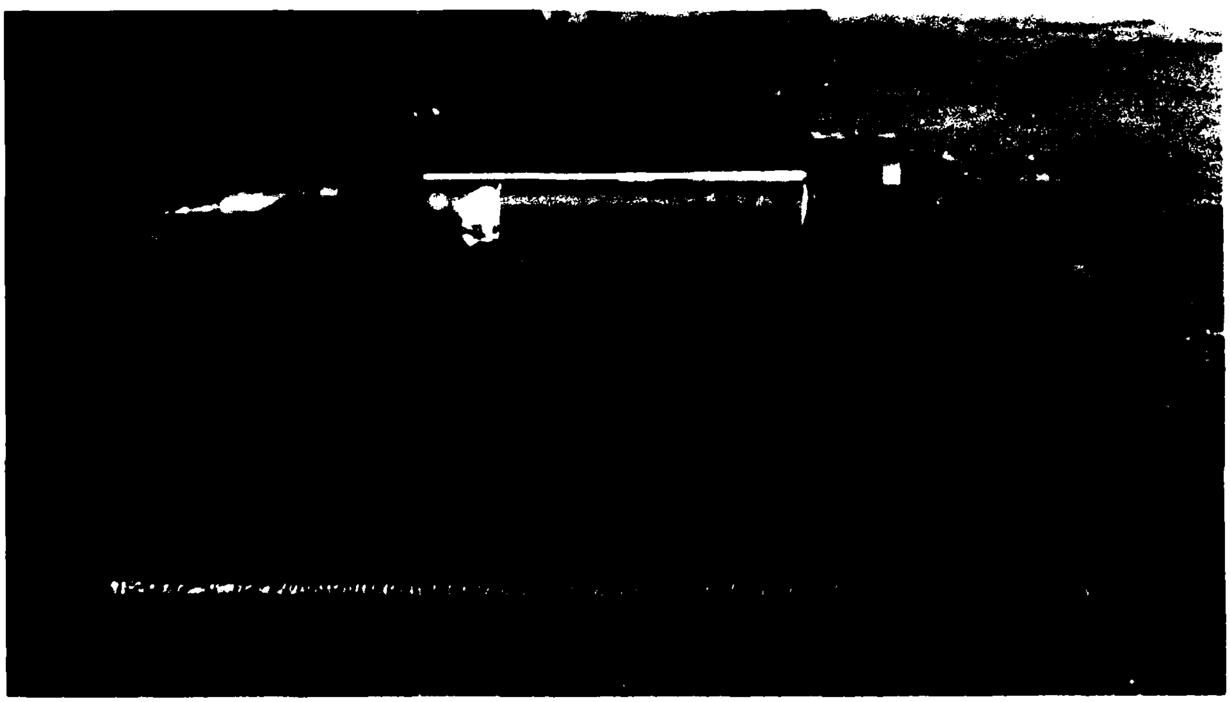

Figure 3. 155-mm Howitzer Simulator

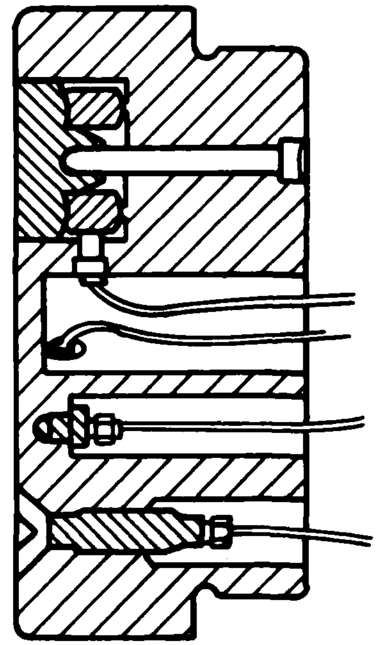

Figure 4. Instrumented Projectile Baseplate

Photographic data were recorded with two high-speed, 16-mm cameras. For each shot, one camera was mounted with a wide angle lens to record the overall aspects of the event and another used a telephoto lens to allow detailed examination of the critical base region of the charge. With all of the cameras, data were recorded at a framing rate of approximately 5000 pictures per second. One-kHz timing signals were placed on the films by electronic circuits internal to the cameras, and the firing fiducial (time at which the firing voltage is applied to the gun) was also placed on the films to aid in correlation of the film data with other data.

Flash radiography was used to monitor the behavior of the solid phase during the interior ballistic cycle. Two 300-kV X-ray heads were employed, aligned perpendicular to the chamber axis and sufficiently separated from each other to allow coverage of the entire chamber length. One image (a "static" shot) was taken of the charge in the chamber before firing, and a second, on a separate film, was recorded during the event by X-rays triggered at a predetermined spindle pressure (a "dynamic" shot). The X-ray film was protected from the blast of the disposable chamber by a wooden cassette, with the forward face composed of layers of air spaces and sacrificial wooden plates.

B. Charge Design

M203E2 Propelling Charges from Lot RDD 83E000E201 were provided by the LCWSL for testing. Each charge contained a single bundle of 737-mm-long slotted sticks from propellant Lot RAD-PE-480-90. The charges were encased in molded nitrocellulose cases, as illustrated in Figure 2. The propellant weight for each charge was 11.85 kg. To facilitate viewing the interior of the charge during the firing event, the combustible case was perforated with a series of windows, measuring 38 mm by 38 mm and spaced on 102 mm centers,

along the length of the case. The windows were covered on the inside of the case with a sheet of plastic 0.38 mm thick, 102 mm wide, and 635 mm long, these dimensions deemed sufficient to support case pressurization while covering a minimum amount of the interior of the case surface. The sheet was glued to the interior of the case with contact cement. Upon reassembly, the charges were restored as nearly as possible to their as-received condition.

Figures 5 and 6 illustrate the two charges fired in this study prior to reassembly. The figures show, in each instance, the single bundle of slotted, single-perforation M31A1E1 propellant, the igniter assembly, and the windowed combustible case. The propellant sticks were coded by several means, most obviously with painted ends, to permit later identification of their location in the charge. Figure 5 shows the charge fired with the perforated separator wall intact. Figure 6 shows the charge with that wall removed. Figure 7 depicts one of the reassembled charges.

III. EXPERIMENTAL RESULTS AND DISCUSSION

The charges were conditioned at 21° C for at least 24 hours prior to firing. Approximately 15 minutes elapsed between the time each of the charges was removed from the conditioning facility and fired. The charges were positioned with a nominal standoff of 25 mm, and initiated with M82 primers. Using pieces of the combustible material, the cases were wedged against the side of the chamber nearest the cameras in order to minimize obscuration of the windows by smoke. After loading, there was an axial distance of approximately 50 mm between the front of the charge and the base of the projectile.

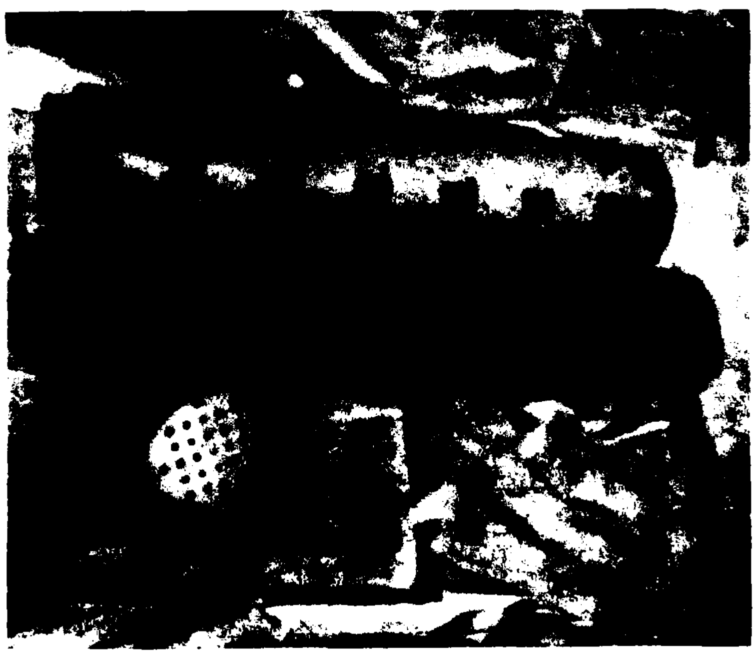

Figure 6. M203E2 Propelling Charge, Peforated Wall Removed

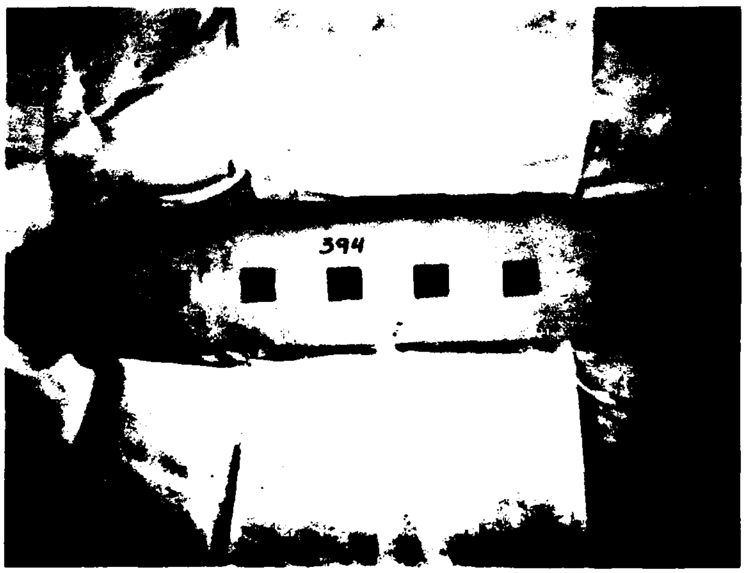

Figure 7. Reassembled M203E2 Propelling Charge

A. <u>M203E2 Charge, Perforated Wall Intact</u>

Figure 8 shows the spindle pressure and projectile-base pressure and force for the M203E2 Charge with the perforated wall left intact prior to firing. The times in the plot are referenced to the instant at which the voltage was applied to the electric firing circuit. The chamber failed at a breech pressure of approximately 7.1 MPa. The breech pressure trace is generally smooth and monotonically increasing, with the only notable detail being the change of slope of the curve at approximately 13 ms. This slope change is perhaps best interpreted in reference to the details seen in the

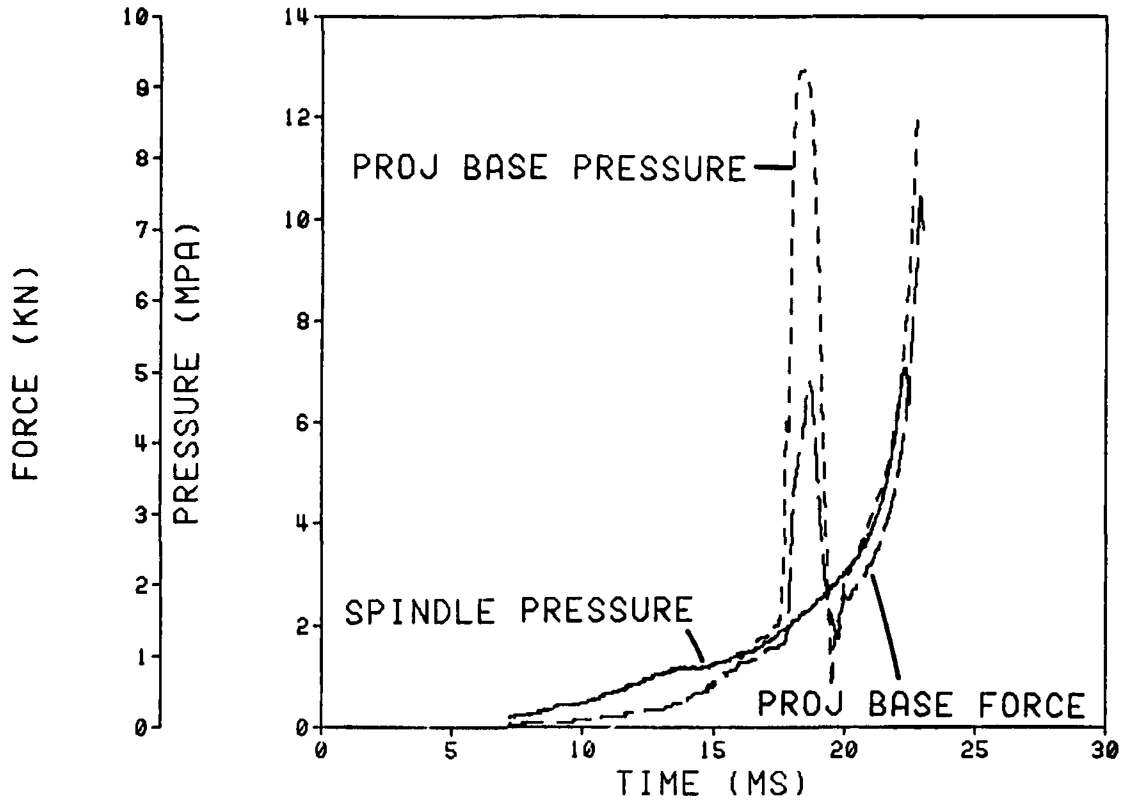

Figure 8. Pressures and Force, M203E2 Propelling Charge, Perforated Wall Intact

high-speed films, addressed below. From the pressure gage on the projectile base, we find a similarly well-behaved trace on which is superimposed a broad spike beginning at about 17.5 ms. The force gage also demonstrates this behavior, and the overall picture is consistent with a steadily rising gas pressure on the base of the projectile, accompanied by an impact of the charge on the projectile base, followed by a rebound of the charge off the projectile base. That the gas-pressure gage responded similarly is likely an artifact of the gage block design, in that a column of gas was trapped between the front of the charge and the gas-pressure gage face. This behavior was seen in the previous tests referenced earlier.[11]

The high-speed films recorded many interesting details of the charge functioning. Figure 9 presents selected frames from both the full-chamber-length and close-up films. In all cases, the spindle is at the left. After the primer functioning, the base igniter began to burn (Figure 9a), and the gases generated such force in the poorly vented igniter cavity that the rear cap popped off the charge (Figure 9b) at about 4 ms. The igniter products continued to vent strongly into the rear ullage with no significant penetration into the propellant bed, as evidenced by the lack of luminosity visible through the charge windows. A portion of the gases escaping the rear of the charge did find their way into the charge through the snap joint (Figures 9b, 9c), however, so that some luminosity was seen in the propellant bed at 13-15 ms, the point at which the spindle pressure showed a slope change. A portion of combustible case surrounding the igniter assembly burned in cigarette

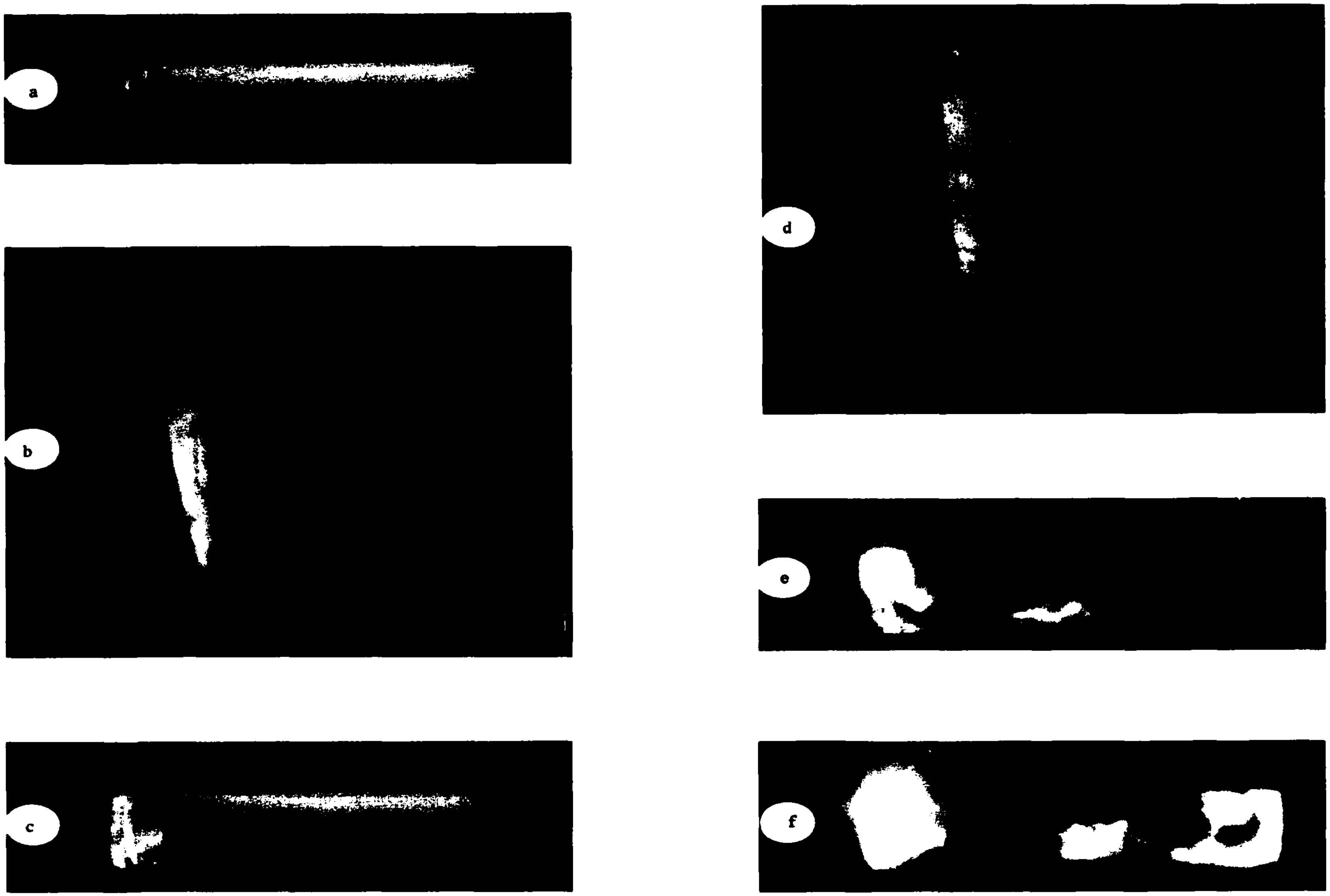

Figure 9. Flamespread, M203E2 Propelling Charge, Perforated Wall Intact

fashion (Figure 9d) during this time, though no well-defined flamespread along any portion of the case was observed. Overall, the high-speed films showed that the igniter and early combustion gases preferentially vented into the ullage (Figure 9e), so much so that gases in the forward ullage pressurized the ullage in that region and then entered the charge through the collapsing forward window of the charge (Figure 9f) before there was significant luminosity along the inside length of the charge.

The triggering circuit of the flash X-ray system was set to operate at a spindle pressure somewhat in excess of 7 MPa. Since the spindle pressure gage failed to reach this level, a dynamic flash X-ray was not obtained for this shot.

B. <u>M203E2 Charge, Perforated Wall Removed</u>

Figure 10 displays the spindle pressure and the projectile-base gas pressure and force recorded from the shot with the igniter modified so that the perforated wall was removed. All of the data were smooth and monotonically increasing until the chamber failed at 12 MPa. Pressurization at the spindle was uniform, again with the slope break noted on the previous shot. Neither the force gage nor the forward pressure gage indicated impact of the charge on the base of the projectile.

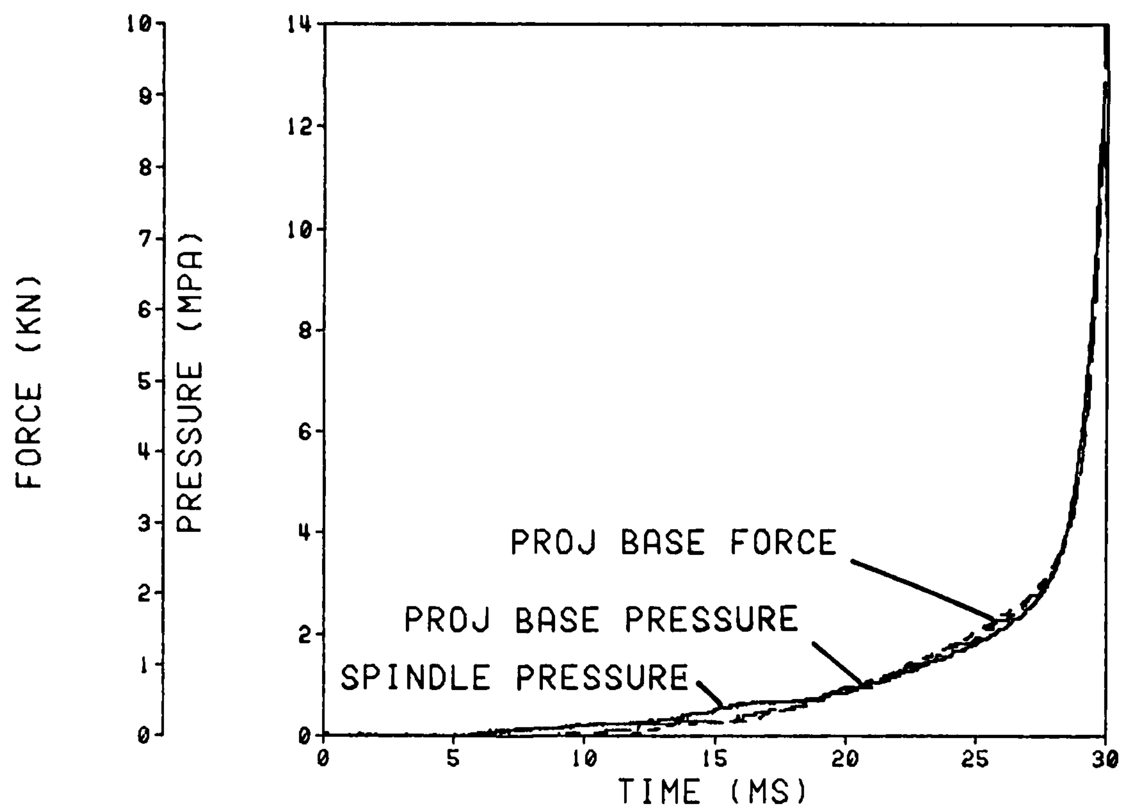

Figure 10. Pressures and Force, M203E2 Propelling Charge, Perforated Wall Removed

The high-speed films for this shot, selected portions of which are shown in Figure 11, revealed details that differ significantly from the previous shot. As in that shot, the basepad began to burn shortly after the primer vented (Figure 11a), but in this instance, the rear charge cap was not forced off the charge (Figure 11b). For the first 5-7 ms, the charge was pushed forward in the chamber by approximately 25 mm, but did not impact the projectile. After about 13 ms, there was considerable luminosity at both ends of the chamber, with no light visible within the charge. Also during this time, gases streaming from the base of the charge appeared to enter the main charge through the snap joint as in the previous shot (Figure 11c). Flame was visible in the rear window at 19 ms, in the front window at 22 ms, and in the next-to-rear window at 24 ms. By about 27 ms, there was more intense flame in these windows (Figure 11d). Shortly thereafter flame filled the interior of the case and the case ruptured longitudinally due to the internal pressurization (Figure 11e).

Figure 12 shows line-drawing schematics of the flash X-rays recorded for this shot. In the static shot recorded in Figure 12a, we note the combustible case, the bed of stick propellant, and the igniter pad. Figure 12b depicts the scene at a spindle pressure of about 7 MPa. We note that the charge was pushed forward, but not completely to impact the projectile. Though not apparent in the high-speed films, the flash X-ray indicates that the base cap was separated from the rear of the case. As an indicator that the case was pressurized from within, we note that the front face was blown off the combustible case. We also note the slight compaction of the ends of the stick propellant bundles in the region where gases enter and leave the propellant bed.

IV. SUMMARY OF MODELING APPROACH

The TDNOVA code was developed to simulate the interior ballistics of single- or multi-increment propelling charges by means of a numerical solution of the equations of two-dimensional, two-phase flow.[12,13] A major effort was recently completed and reported by Gough[14] to extend the TDNOVA code to permit the simulation of stick propellant charges in combustible cases. Under this representation, the charge is assumed to consist of a number of increments of similar but not necessarily identical diameters, loaded end-to-end. Each increment is assumed to be separately enclosed in a container which may be either a flexible bag or a rigidized case. The segments of each container may

---

[12] P.S. Gough, "A Two-Dimensional Model of the Interior Ballistics of Bagged Artillery Charges," ARBRL-CR-00452, Ballistic Research Laboratory, USA ARRADCOM, Aberdeen Proving Ground, MD, April 1981 (AD A100751).

[13] P.S. Gough, "Two-Dimensional, Two-Phase Modeling of Multi-Increment Bagged Artillery Charges," ARBRL-CR-00503, Ballistic Research Laboratory, USA ARRADCOM, Aberdeen Proving Ground, MD, February 1983 (AD A125482).

[14] P.S. Gough, "Modeling of Rigidized Gun Propelling Charges," ARBRL-CR-00518, Ballistic Research Laboratory, USA ARRADCOM, Aberdeen Proving Ground, MD, November 1983 (AD A135860).

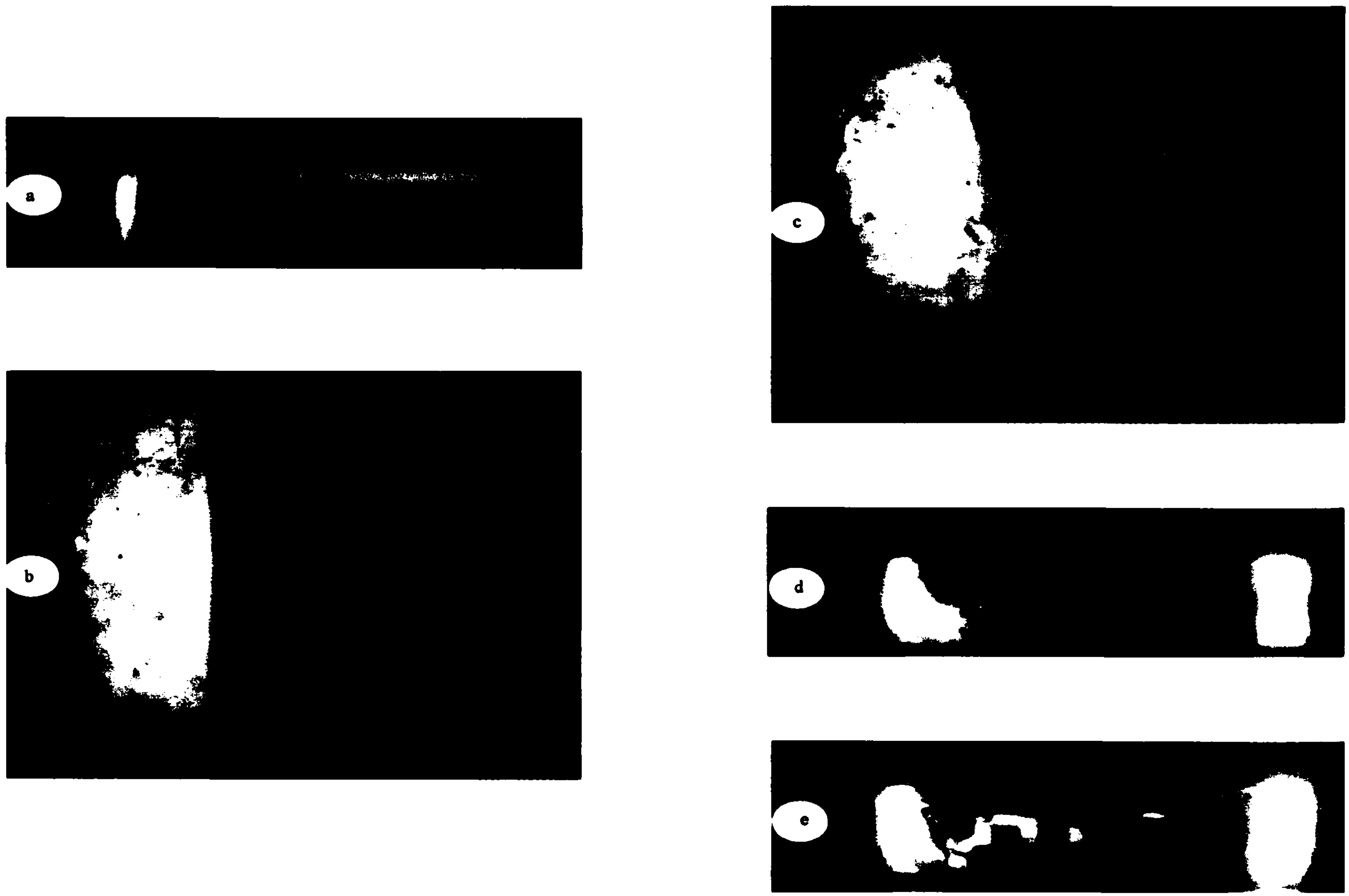

Figure 11. Flamespread, M203E2 Propelling Charge, Perforated Wall Removed

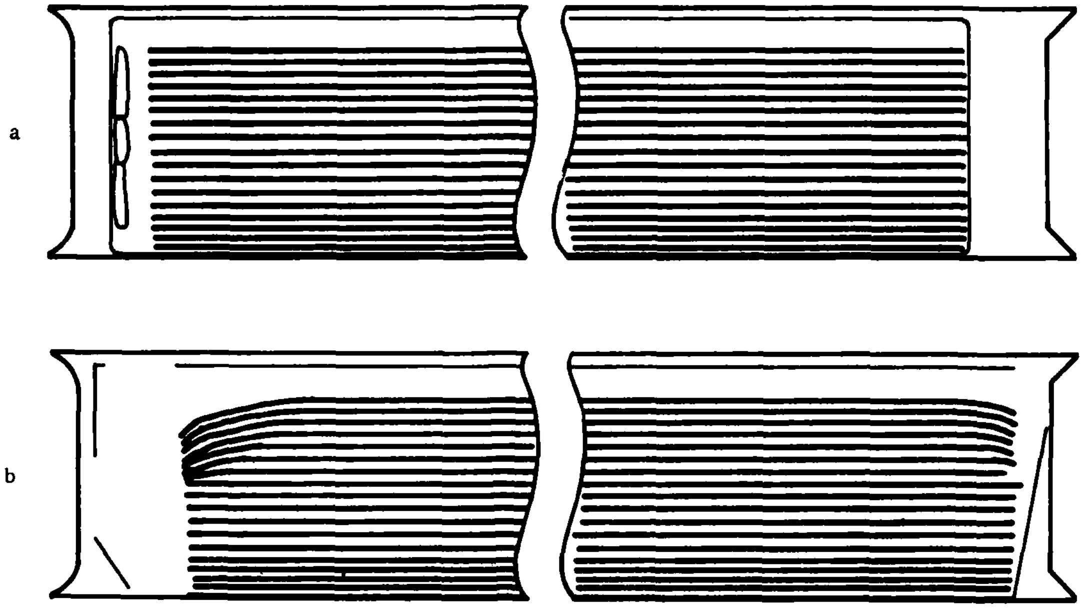

Figure 12. Flash X-ray Schematic Drawings, M203E2 Propelling Charge, Perforated Wall Removed (a) Static (b) Spindle Pressure 7 MPa

be characterized as having two reactive substrates on either side, permitting the simulation of combustion on either side of the container, as well as an additional component, such as a basepad, attached to the surface. Each increment may also incorporate a centercore igniter which is modeled as a quasi-one-dimensional, two-phase flow. The main charge of each increment may be either granular or stick propellant. Stick propellant may be unperforated, perforated, or perforated and slotted. A dual-voidage representation is made of perforated stick propellant; the state of the gas in the perforations is assumed to differ from that in the interstices. The code similarly distinguishes between the exterior and interior surface temperatures and combustion rates of perforated stick propellant. Further, the interphase drag and heat transfer and the solid-phase stress tensor for the stick charges are all posed in terms of anisotropic laws.

The ballistic consequences of heat loss to the tube may be evaluated by means of models based on steady-state pipe and plate flow correlations or by reference to an unsteady boundary layer model. Other constitutive extensions to the code include the influence of erosive burning, flow resistance in narrow regions of ullage, slow gas-phase kinetics with partial heat release at the surface of the solid phase, and a revision to the interphase drag correlation for granular propellant.

Each main charge increment is modeled as a two-dimensional, two-phase flow until flamespreading is complete, all containers are fully ruptured, and radial pressure gradients have subsided to within some user-selectable tolerance. Subsequently, a quasi-two-dimensional representation, in which the propelling charge and the region of circumferential ullage are treated as coupled regions of quasi-one-dimensional flow, is effected to complete the simulation of the interior ballistic cycle in an economical manner. The only exception is for the igniter increment, which, because of the likelihood of severe mesh

distortion and strain on the numerics, is incorporated into the rear region of ullage when either burnout or compression to 10% of its original axial extent occurs locally. The overall solution is obtained by means of an explicit, two-step marching scheme for all interior mesh points together with characteristic forms at the external boundaries defined by the chamber and projectile and at the internal boundaries defined by the interfaces between the mixture and the ullage. The physical role played by the containers of the increments, including reactivity, resistance to penetration by the gas phase, and confinement of the solid phase, is reflected in the model by reference to internal boundary conditions.

V. THEORETICAL RESULTS AND DISCUSSION

We now address application of the TDNOVA code to the M203E2 Propelling Charge by reference to the schematic of Figure 13. The overall approach was in general agreement with that reported previously,[15] though subsequent improvements to the code as well as modifications to the treatment of the igniter increment enabled the calculations to be carried to completion with far fewer compromises to the input data. The exterior boundary depicted an axisymmetric representation of the gun chamber, including spindle face at the breech end and projectile at the forward end. The centerline, breech end, and sidewall remained fixed boundaries, while projectile motion in response to the burning propellant charge was resisted by an independently determined projectile engraving/bore resistance profile.

Internal boundaries reflected packaging of the individual increments -- in this case, the igniter region and the main charge compartment. Mechanical

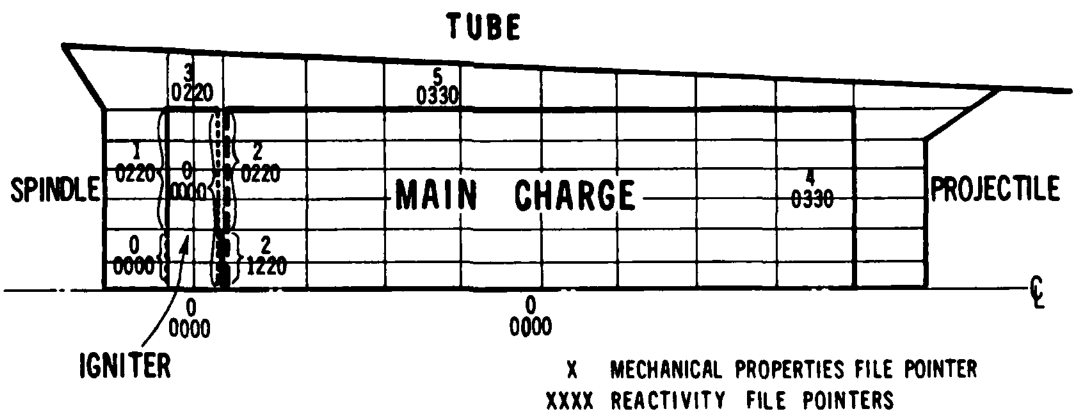

Figure 13. TDNOVA Representation of the M203E2 Propelling Charge

[15]A.W. Horst, F.W. Robbins, and P.S. Gough, "Multidimensional, Multiphase Flow Analysis of Flamespreading in a Stick Propellant Charge," ARBRL-MR-03372, Ballistic Research Laboratory, ARDC, USA AMCCOM, August 1984 (AD A145731).

properties of each segment of the container were identified by a single-digit number which pointed to an input file providing information on permeability, strength, and related parameters. Corresponding reactivity characteristics for each segment were indicated by a four-digit number, identifying files describing gasification rates and thermodynamic parameters associated with each of the inner and outer surfaces and attached components as described above. The small black powder charge in the igniter increment was treated here as an attached component described by reactivity file #1. The earlier analysis of this charge[15] assumed the black powder charge to be attached to the interior of a permeable boundary separating the igniter and main charge regions, but attached to the igniter increment. In the present calculations, we assumed this boundary element, including the black powder charge, to be a part of the main charge, so that its influence was not lost when the igniter increment was incorporated into the region of rear ullage upon severe mesh distortion or local burnout.

In addition, propellant input files were specified for the CBI material and the M31-type stick propellant to describe mechanical properties, dimensions, thermal properties of the solid, ignition and combustion characteristics, and thermodynamic properties of the product gases. Corresponding files for the various combustible case materials were also included since explicit modeling of ig..ition and combustion of the case was of interest.

We turn now to the results from a TDNOVA calculation based on a nominal input data base for the M203E2 Propelling Charge. The process began, in the calculation, with the rapid burning of the black powder spot, in accordance with a tabular description provided as input. Thus, all delays associated with the functioning of the primer prior to ignition of the basepad were outside the scope of the simulation. Combustion gases from the burning black powder rapidly ignited the main CBI charge in the igniter increment, locally pressurizing this region of the charge, as shown in Figure 14. For a little more than the next millisecond, the combined products of the black powder and CBI charges pressurized the regions of ullage behind and circumferentially external to the charge as well. Interestingly enough, however, little pressurization within the main body of the charge took place during this early period. While it is true that the sidewall of the charge was initially impermeable, the wall separating the two increments was intentionally perforated to allow early passage of igniter products to promote rapid ignition of the main charge of stick propellant. Nevertheless, the perforated area represented less than 20 percent of the total area and was apparently altogether insufficient for this purpose.

The accompanying gas flow is depicted in Figure 15. (Flow vectors originate at the centers of the cells and are normalized with respect to the largest value of velocity at that particular time.) A substantial portion of early igniter products flowed rearward and around the case, a path that apparently presented far less resistance than did the path through the perforated wall into the bundle of stick propellant. As shown in Figure 16, the small CBI particles were carried along as well, leading to a significant distortion of the mesh associated with the igniter increment. It is at this point that previous attempts to simulate the M203E2 Charge with TDNOVA failed, despite the use of an artificially stiff representation of the CBI bed rheology. However, in the current calculation, igniter burnout occurred locally at 2.778 ms into the calculation, the igniter region was incorporated into the rear

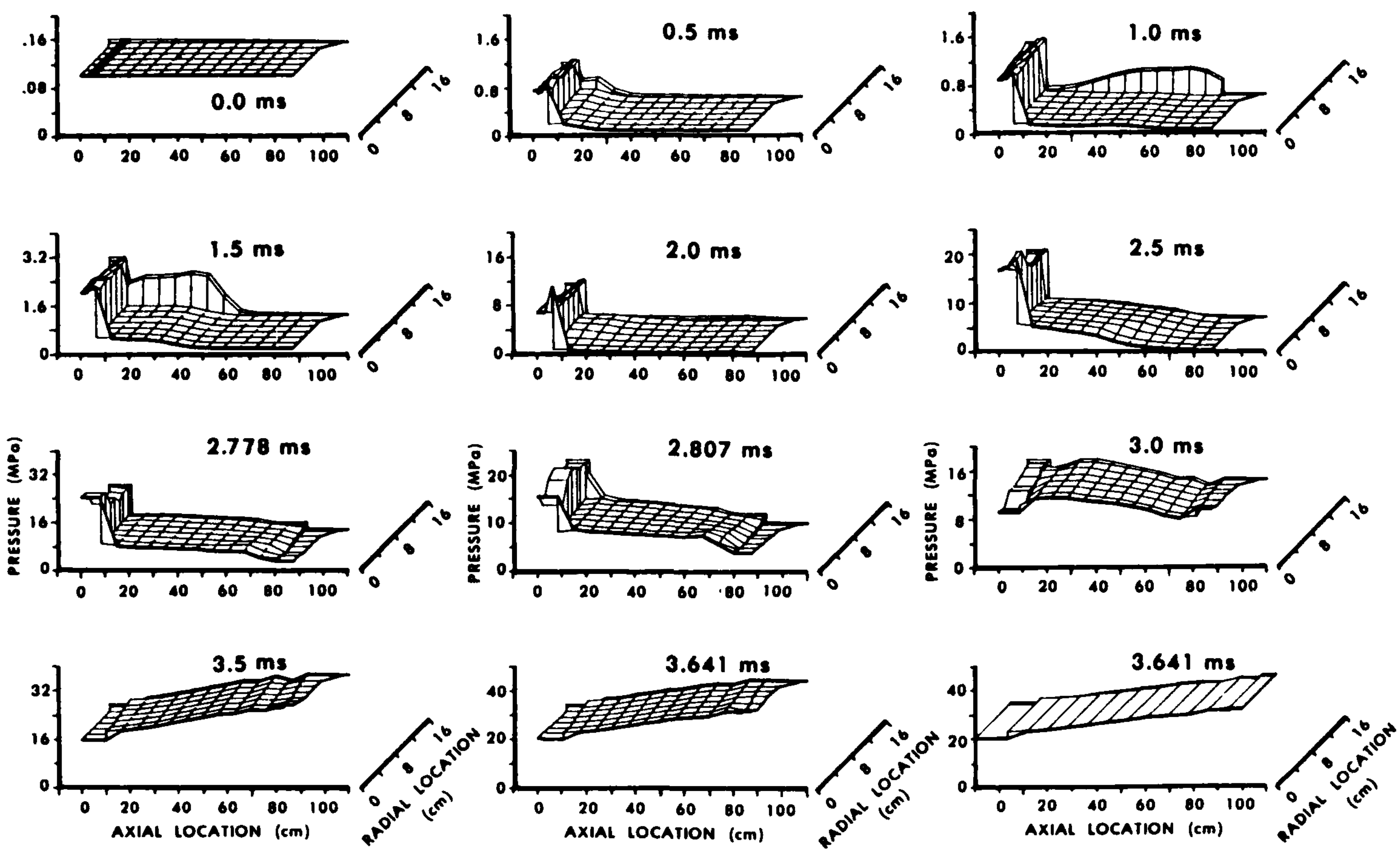

Figure 14. Predicted Pressure Fields for the M203E2 Propelling Charge

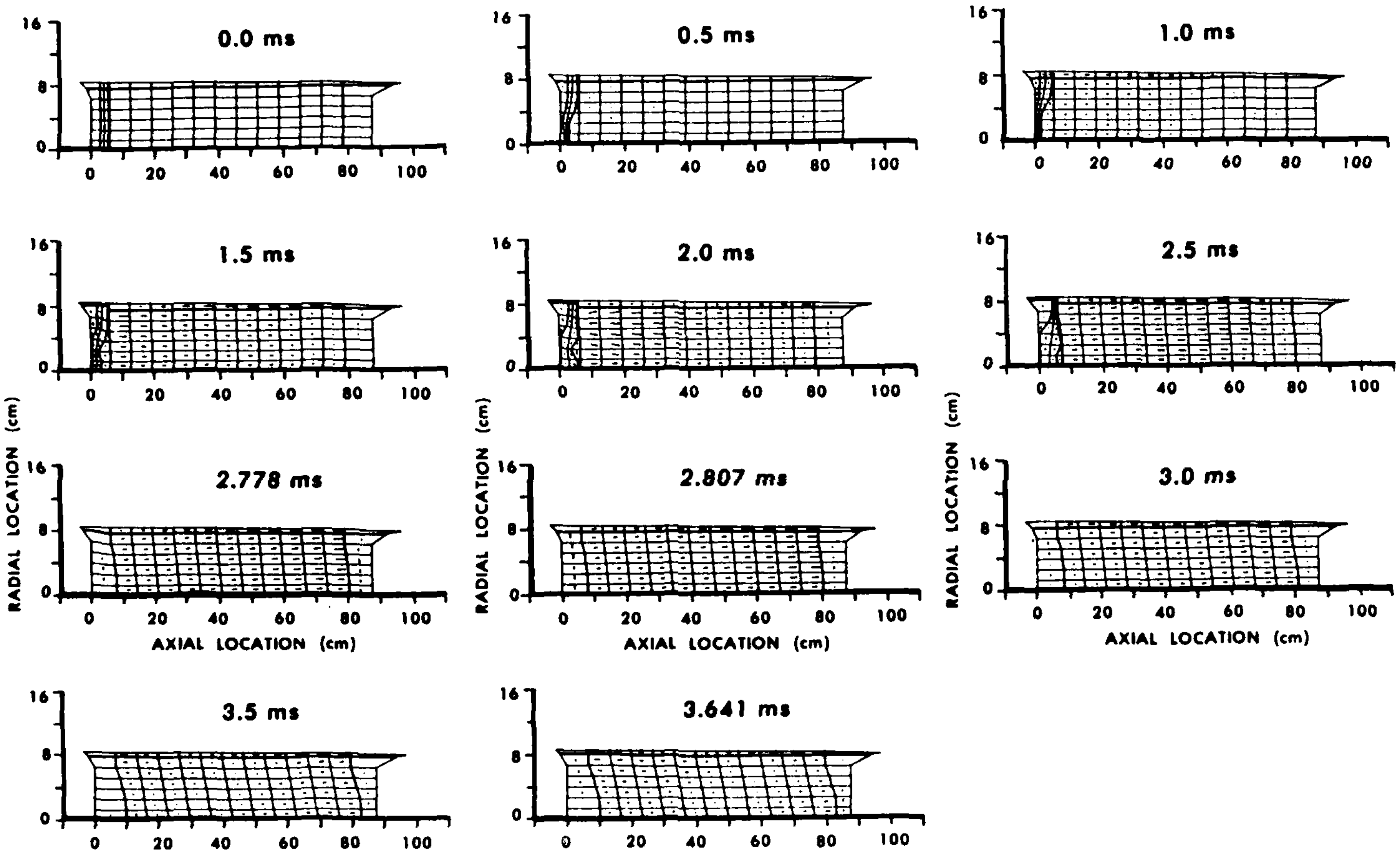

Figure 15. Predicted Gas-Phase Flow Fields for the M203E2 Propelling Charge

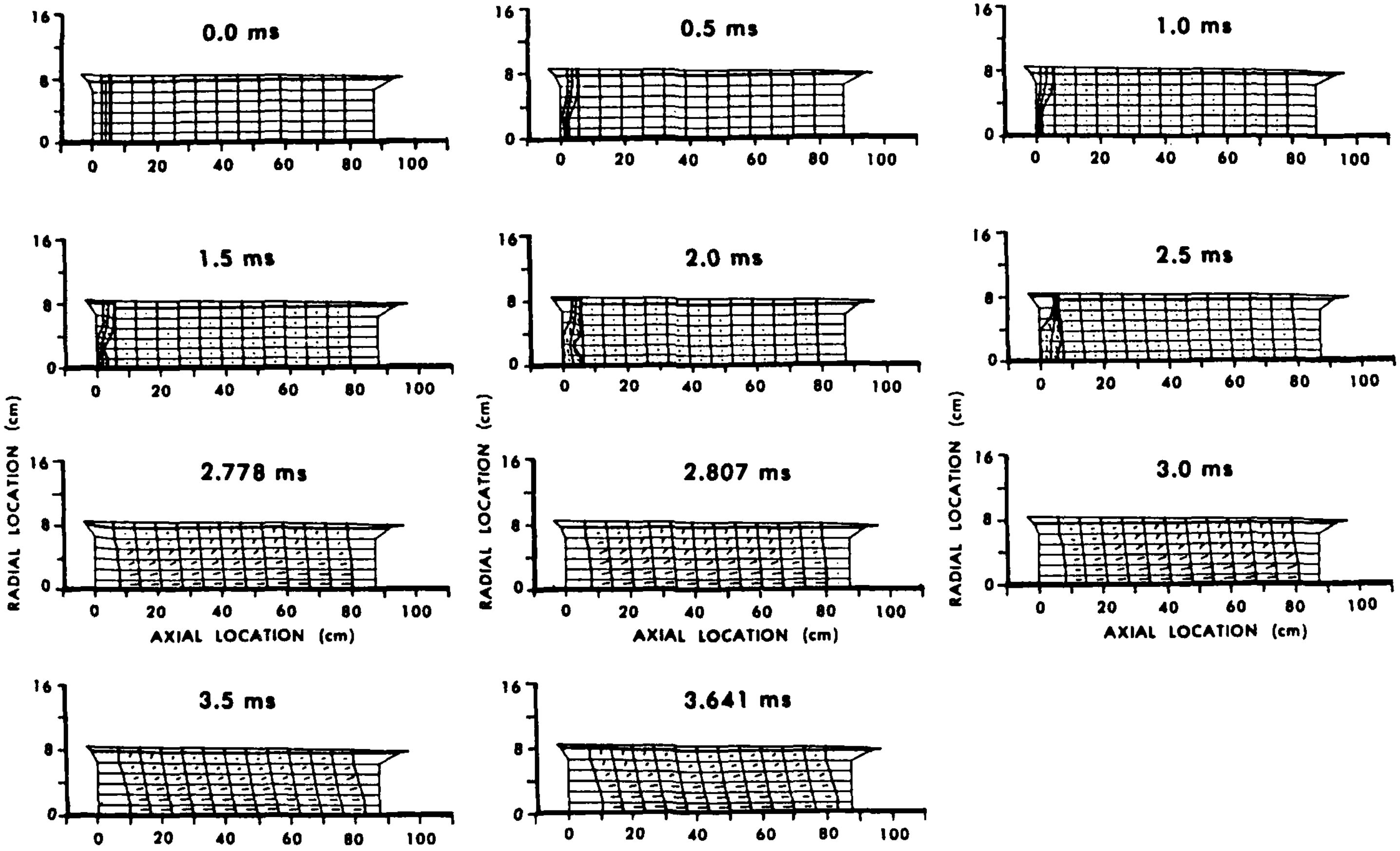

Figure 16. Predicted Solid-Phase Flow Fields for the M203E2 Propelling Charge

continuum of ullage, and the calculation marched on. With the perforated wall assumed to be a part of the main increment, its permeability and energy release characteristics continued to influence the calculation despite the loss of any remaining CBI. Ignition of the main charge of stick propellant began adjacent to the igniter increment at about 1.5 ms into the calculation and proceeded, via a nearly one-dimensional process, to completion some 1.3 ms later. Little difference was seen between external and internal surfaces of the sticks since the propellant was slotted and the slots were assumed to be initially open. The dual-voidage representation of the propellant was then dropped in favor of a more economical single-voidage model which assumed interstitial and perforation conditions to be locally the same. This transformation would not have taken place at this point were the propellant unslotted or the slots assumed to be closed until a specified internal overpressure was reached. A final transformation to the quasi-two-dimensional representation was made at 3.641 ms into the calculation, when radial pressure gradients at each axial station fell to less than 5 percent of the pressure at the centerline.

In the calculation, flamespreading up the external sidewall of the case preceded flamespreading through the bundle of sticks by about a millisecond. While the importance of this result on the overall ignition process remains to be examined in detail, we caution the reader that ignition and combustion characteristics for the case material were, in many respects, only estimated in order to permit the current set of calculations. Despite the paucity of data, however, linkages within the code to permit simulation of flamespreading along the case via convective processes were tested and warrant future exploitation to investigate physical significance. Similarly, in respect to case rupture, the lack of a good mechanical description of the combustible cartridge case in the reacting, dynamic gun environment must limit the value of our results in the absolute sense. The current calculation was based on a linear elastic model of the case sidewall, with local failure based on a von Mises equivalent stress for the sidewall and a simple overpressure criterion for the ends. Using this representation and estimated values for the appropriate parameters, the igniter increment began to rupture almost immediately due to rapid internal pressurization. Failure of the main charge case increment appeared to follow the local pressurization associated with passage of the combustion front through the sticks during flamespreading, though the forward end was blown out nearly a millisecond before the flame reached it.

A second calculation was performed with the effective flow area of the perforated wall cut in half, further restricting the early passage of igniter gases into the main charge. The result was more early flow around the outside of the charge, speeding the propagation of flame up the outer sidewall of the case but delaying flamespreading through the main stick charge by more than half a millisecond. Moreover, the forward velocity imparted to the charge during this early phase was more than doubled, resulting in the charge striking the base of the projectile at about 20 m/s.

A final calculation was attempted with the wall represented as being totally permeable. As expected, flame propagation up the outside of the case was slowed appreciably, but flamespreading through the main charge stalled, rather than being accelerated. The only explanation we can suggest at this time is that, without the pressure differential built up across the perforated wall, the blowing process was mitigated and convective heat transfer to the propellant dropped below the critical level required to achieve ignition.

VI. CONCLUSIONS

This combined experimental/theoretical study provides us with considerable insight into the phenomenology of flamespreading in a combustible-cased, stick propellant charge. In particular, the case was shown to exert substantial influence on the early path of flamespreading, the perforated wall between the igniter and main stick charge blocking most of the igniter gases from directly entering the main charge as intended. The separation of igniter components from the rest of the charge, revealed in the films, was confirmed in the calculations to be a result of the rearward path of the igniter gases, filling the region of ullage behind the charge and then propagating up the circumferential ullage adjacent to the charge sidewall. This preferential flow of igniter gases, again clearly shown in the films, was predicted in the calculations to lead to locally higher pressures external to the charge, the magnitude of which depended on the initial flow area of the perforated wall. Such locally excessive pressures external to the charge were no doubt responsible for both the previously observed radial compaction of the charge and current results, theoretical and experimental, revealing forward motion of the charge during flamespread, both phenomena appearing to be directly influenced by the configuration of the perforated wall.

We should emphasize, however, that not all of the resistance to igniter gas entry into the main charge results from the barrier imposed by the combustible case. While natural flow channels <u>within</u> the bundle of sticks offer little resistance to the axial flow of gases, entrance conditions at the end of the tightly packed bundle provide quite an impediment to the <u>entering</u> gases, as evidenced in both the film and the calculation by the substantial flow of igniter gases external to the charge even when the perforated wall was absent. An interesting experimental result, outside the scope of the simulations, was the subsequent yet potentially significant re-entry of igniter gases into the charge, this time on the far side of the perforated wall through a snap joint in the case. This initial breaching of the otherwise impermeable case sidewall, presumably a result of minor crushing of the rear portion of the case by external pressures, may have provided the principal path for the entrance of igniter gases into the main charge of stick propellant. We note that, except at this assembly joint, the mechanical integrity of the case sidewall apparently persists until flamespreading within the main charge sufficiently elevates internal pressures beyond those in the ullage for rupture to occur. Hence, the impermeability of the sidewall to igniter gases in the ullage and the confinement of the sticks until case rupture can both be expected to play major roles in characterizing the path of flamespread.

It was noted that the calculations revealed that flamespread up the exterior of the case commenced prior to that in the main charge of stick propellant. No well-defined flamespread along the case sidewall, however, was

observed in the experiments, though burning of the rear portion of the case was clearly seen in one of the films. Moreover, flamespread within the bundle of stick propellant was never clearly defined in the films, but rather seemed to engulf the entire charge nearly simultaneously after a few [illegible] seconds during which it was presumably bathed in hot igniter gases. [illegible] revealed ignition of the base of the sticks after a [illegible] igniter functioning, followed by a brief hesitation, and [illegible] spreading at an approximately uniform rate nearly twice that [illegible] propellant charges providing comparable ballistic [illegible] appar- ently this near simultaneity of ignition of the [illegible] charge, regardless of the details of the ignition stimulus [illegible] an amazing insensitivity of ballistic performance to a [illegible] compo- sitions and configurations demonstrated in recent [illegible] Charge.

Overall, this study has confirmed the complexity of the interplay among the igniter, propellant, and cartridge case for combustible cased, stick propellant charges. For the propelling charge developer, these features all represent exploitable charge design parameters, potentially capable of influ- encing safety, reliability, and performance. We further view it as the responsibility of the research community to advance modeling and experimental diagnostic capabilities such as those employed in this study to facilitate the task of the charge developer.

ACKNOWLEDGMENTS

The authors wish to thank Dr. P.S. Gough of *Paul Gough Associates*, Inc., Portsmouth, NH, for his valuable assistance in application of the TDNOVA code to the problem of interest and Mr. O. Colitti, ARDC, Dover, NJ, who provided the M203E2 Propelling Charges used in this investigation.

REFERENCES

1. S. Weiner, "Investigation of Stick Propellant for 155-mm, XM198," Interim Memorandum Report, Picatinny Arsenal, Dover, NJ, July 1975.

2. T.C. Smith, "Experimental Gun Testing of High Density Multiperforated Stick Propellant Charge Assemblies," 17th JANNAF Combustion Meeting, CPIA Publication 329, Vol. II, pp. 119-124, November 1980.

3. F.W. Robbins, J.A. Kudzal, J.A. McWilliams, and P.S. Gough, "Experimental Determination of Stick Charge Flow Resistance," 17th JANNAF Combustion Meeting, CPIA Publication 329, Vol. II, pp. 97-118, November 1983.

4. T.C. Minor, "Mitigation of Ignition-Induced, Two-Phase Flow Dynamics Through the Use of Stick Propellants," ARBRL-TR-02508, Ballistic Research Laboratory, USA ARRADCOM, Aberdeen Proving Ground, MD, August 1980 (AD A133685).

5. A.W. Horst, "A Comparison of Barrel-Heating Processes for Granular and Stick Propellant Charges," ARBRL-MR-03193, Ballistic Research Laboratory, USA ARRADCOM, Aberdeen Proving Ground, MD, August 1982 (AD A118394).

6. F.W. Robbins and A.W. Horst, "Slotted Stick Propellant Study," 20th JANNAF Combustion Meeting, CPIA Publication 383, Vol. I, pp. 377-386, October 1983.

7. A.W. Horst and T.C. Minor, "Ignition-Induced Flow Dynamics in Bagged-Charge Artillery," ARBRL-TR-02257, Ballistic Research Laboratory, USA ARRADCOM, Aberdeen Proving Ground, MD, August 1980 (AD A090681).

8. A.W. Horst and P.S. Gough, "Modeling Ignition and Flamespread Phenomena in Bagged Artillery Charges," ARBRL-TR-02263, Ballistic Research Laboratory, USA ARRADCOM, Aberdeen Proving Ground, MD, September 1980 (AD A091790).

9. A.W. Horst, F.W. Robbins, and P.S. Gough, "A Two-Dimensional, Two-Phase Flow Simulation of Ignition, Flamespread, and Pressure-Wave Phenomena in the 155-mm Howitzer," ARBRL-TR-02414, Ballistic Research Laboratory, USA ARRADCOM, Aberdeen Proving Ground, MD, July 1982 (AD A119148).

10. T.C. Minor, "Experimental Studies of Multidimensional Two-Phase Flow Processes in Interior Ballistics," ARBRL-MR-03248, Ballistic Research Laboratory, USA ARRADCOM, Aberdeen Proving Ground, MD, April 1983 (AD A128034).

11. T.C. Minor and A.W. Horst, "Ignition Phenomena in Developmental, Stick-Propellant, Combustible-Cased, 155-mm, M203E2 Propelling Charges," ARBRL-TR-02568, Ballistic Research Laboratory, ARDC, USA AMCCOM, Aberdeen Proving Ground, MD, July 1984 (AD A145283).

12. P.S. Gough, "A Two-Dimensional Model of the Interior Ballistics of Bagged Artillery Charges," ARBRL-CR-00452, Ballistic Research Laboratory, USA ARRADCOM, Aberdeen Proving Ground, MD, April 1981 (AD A100751).

13. P.S. Gough, "Two-Dimensional, Two-Phase Modeling of Multi-Increment Bagged Artillery Charges," ARBRL-CR-00503, Ballistic Research Laboratory, USA ARRADCOM, Aberdeen Proving Ground, MD, February 1983 (AD A125482).

14. P.S. Gough, "Modeling of Rigidized Gun Propelling Charges," ARBRL-CR-00518, Ballistic Research Laboratory, USA ARRADCOM, Aberdeen Proving Ground, MD, November 1983 (AD A135860).

15. A.W. Horst, F.W. Robbins, and P.S. Gough, "Multidimensional, Multiphase Flow Analysis of Flamespreading in a Stick Propellant Charge," ARBRL-MR-03372, Ballistic Research Laboratory, ARDC, USA AMCCOM, August 1984 (AD A145731).

DISTRIBUTION LIST

No. Of Copies	Organization
12	Administrator Defense Technical Info Center ATTN: DTIC-DDA Cameron Station Alexandria, VA 22304-6145
1	Commander USA Concepts Analysis Agency ATTN; D. Hardison 8120 Woodmont Avenue Bethesda, MD 20014-2797
1	HQDA/DAMA-ZA Washington, DC 20310-2500
1	HQDA, DAMA-CSM, E. Lippi Washington, DC 20310-2500
1	HQDA/SARDA Washington, DC 20310-2500
1	Commander US Army War College ATTN: Library-FF229 Carlisle Barracks, PA 17013
1	US Army Ballistic Missile Defense Systems Command Advanced Technology Center P. O. Box 1500 Huntsville, AL 35807-3801
1	Chairman DOD Explosives Safety Board Room 856-C Hoffman Bldg. 1 2461 Eisenhower Avenue Alexandria, VA 22331-9999
1	Commander US Army Materiel Command ATTN: AMCPM-GCM-WF 5001 Eisenhower Avenue Alexandria, VA 22333-0001

No. Of Copies	Organization
1	Commander US Army Materiel Command ATTN: AMCDRA-ST 5001 Eisenhower Avenue Alexandria, VA 22333- 0001
1	Commander US Army Materiel Command ATTN: AMCDE-DW 5001 Eisenhower Avenue Alexandria, VA 22333- 0001
5	Project Manager Cannon Artillery Weapons System, ARDC, AMCCOM ATTN: AMCPM-CW, F. Menke AMCPM-CWW AMCPM-CWS M. Fisette AMCPM-CWA R. DeKleine H. Hassmann Dover, NJ 07801-5001
2	Project Manager Munitions Production Base Modernization and Expansion ATTN: AMCPM-PBM, A. Siklosi AMCPM-PBM-E, L. Laibson Dover, NJ 07801-5001
3	Project Manager Tank Main Armament System ATTN: AMCPM-TMA, K. Russell AMCPM-TMA-105 AMCPM-TMA-120 Dover, NJ 07801-5001
1	Commander US Army Watervliet Arsenal ATTN: SARWV-RD, R. Thierry Watervliet, NY 12189

DISTRIBUTION LIST

No. Of Copies	Organization
20	Commander US Army ARDC, AMCCOM ATTN: SMCAR-TSS SMCAR-TDC SMCAR-LC LTC N. Barron SMCAR-LCA A. Beardell D. Downs S. Einstein S. Westley S. Bernstein C. Roller J. Rutkowski SMCAR-LCB-I D. Spring SMCAR-LCE SMCAR-LCM-E S. Kaplowitz SMCAR-LCS SMCAR-LCU-CT E. Barrieres R. Davitt SMCAR-LCU-CV C. Mandala SMCAR-LCW-A M. Salsbury SMCAR-SCA L. Stiefel B. Brodman Dover, NJ 07801
4	Commander US Army Armament Munitions and Chemical Command ATTN: SMCAR-ESP-L Rock Island, IL 61299-7300
1	HQDA DAMA-ART-M Washington, DC 20310-2500
1	Director Benet Weapons Laboratory Armament R&D Center US Army AMCCOM ATTN: SMCAR-LCB-TL Watervliet, NY 12189
1	Commander US Army Aviation Research and Development Command ATTN: AMSAV-E 4300 Goodfellow Blvd. St. Louis, MO 63120-1702
1	Commander US Army TSARCOM 4300 Goodfellow Blvd. St. Louis, MO 63120-1702
1	Director US Army Air Mobility Research And Development Laboratory Ames Research Center Moffett Field, CA 94035-1099
1	Commander US Army Communications - Electronics Command ATTN: AMSEL-ED Fort Monmouth, NJ 07703-5301
1	Commander ERADCOM Technical Library ATTN: DELSD-L (Report Section) Fort Monmouth, NJ 07703-5301
1	Commander US Army Harry Diamond Lab. ATTN: DELHD-TA-L 2800 Powder Mill Road Adelphi, MD 20783-1145
1	Commander US Army Missile Command ATTN: AMSMI-CM Redstone Arsenal, AL 35898-5249

DISTRIBUTION LIST

No. Of Copies	Organization
1	Commander, U.S. Army Missile Command, Research, Development & Engineering Center ATTN: AMSMI-RD Redstone Arsenal, AL 35898
1	Director, U.S. Army Missile & Space Intelligence Center ATTN: AIAMS-YDL Redstone Arsenal, AL 35898-5500
1	Commandant US Army Aviation School ATTN: Aviation Agency Fort Rucker, AL 36360
1	Commander US Army Tank Automotive Command ATTN: AMSTA-TSL Warren, MI 48092-2498
1	Commander US Army Tank Automotive Command ATTN: AMSTA-CG Warren, MI 48092-2498
1	Project Manager Improved TOW Vehicle ATTN: AMCPM-ITV US Army Tank Automotive Command Warren, MI 48092-2498
2	Program Manager M1 Abrams Tank System ATTN: AMCPM-GMC-SA, T. Dean Warren, MI 48092-2498
1	Project Manager Fighting Vehicle Systems ATTN: AMCPM-FVS Warren, MI 48092-2498

No. Of Copies	Organization
1	President US Army Armor & Engineer Board ATTN: ATZK-AD-S Fort Knox, KY 40121-5200
1	Project Manager M-60 Tank Development ATTN: AMCPM-M60TD Warren, MI 48092-2498
1	Director US Army TRADOC Systems Analysis Activity ATTN: ATAA-SL White Sands Missile Range, NM 88002
1	Commander US Army Training & Doctrine Command ATTN: ATCD-MA/ MAJ Williams Fort Monroe, VA 23651
1	Commander US Army Materials and Mechanics Research Center ATTN: AMXMR-ATL Tech Library Watertown, MA 02172
1	Commander US Army Research Office ATTN: Tech Library P. O. Box 12211 Research Triangle Park, NC 27709-2211
1	Commander US Army Belvoir Research & Development Center ATTN: STRBE-WC Fort Belvoir, VA 22060-5606

DISTRIBUTION LIST

No. Of Copies	Organization
1	Commander US Army Logistics Mgmt Ctr Defense Logistics Studies Fort Lee, VA 23801
1	Commandant US Army Infantry School ATTN: ATSH-CD-CSO-OR Fort Benning, GA 31905
1	President US Army Artillery Board Ft. Sill, OK 73503-5600
1	Commandant US Army Command and General Staff College Fort Leavenworth, KS 66027
1	Commandant US Army Special Warfare School ATTN: Rev & Tng Lit Div Fort Bragg, NC 28307
1	Commander Radford Army Ammunition Plant ATTN: SMCRA-QA/HI LIB Radford, VA 24141-0298
1	Commander US Army Foreign Science & Technology Center ATTN: AMXST-MC-3 220 Seventh Street, NE Charlottesville, VA 22901-5396
1	Commandant US Army Field Artillery Center & School ATTN: ATSF-CO-MW, B. Willis Ft. Sill, OK 73503-5600
1	Commander US Army Development and Employment Agency ATTN: MODE-TED-SAB Fort Lewis, WA 98433

No. Of Copies	Organization
1	Chief of Naval Material Department of the Navy Arlington, VA 20360
1	Office of Naval Research ATTN: Code 473, R. S. Miller 800 N. Quincy Street Arlington, VA 22217-9999
3	Commandant US Army Armor School ATTN: ATZK-CD-MS M. Falkovitch Armor Agency Fort Knox, KY 40121-5215
2	Commander Naval Sea Systems Command ATTN: SEA 62R SEA 64 Washington, DC 20362-5101
1	Commander Naval Air Systems Command ATTN: AIR-954-Tech Lib Washington, DC 20360
1	Assistant Secretary of the Navy (R, E, and S) ATTN: R. Reichenbach Room 5E787 Pentagon Bldg. Washington, DC 20350
1	Naval Research Lab Tech Library Washington, DC 20375
5	Commander Naval Surface Weapons Center ATTN: Code G33, J. L. East W. Burrell J. Johndrow Code G23, D. McClure Code DX-21 Tech Lib Dahlgren, VA 22448-5000

DISTRIBUTION LIST

No. Of Copies	Organization
2	Commander US Naval Surface Weapons Center ATTN: J. P. Consaga C. Gotzmer Indian Head, MD 20640-5000
4	Commander Naval Surface Weapons Center ATTN: S. Jacobs/Code 240 Code 730 K. Kim/Code R-13 R. Bernecker Silver Spring, MD 20903-5000
2	Commanding Officer Naval Underwater Systems Center Energy Conversion Dept. ATTN: CODE 5B331, R. S. Lazar Tech Lib Newport, RI 02840
4	Commander Naval Weapons Center ATTN: Code 388, R. L. Derr C. F. Price T. Boggs Info. Sci. Div. China Lake, CA 93555-6001
1	Superintendent Naval Postgraduate School Dept. of Mechanical Engineering Monterey, CA 93943-5100
1	Program Manager AFOSR Directorate of Aerospace Sciences ATTN: L. H. Caveny Bolling AFB, DC 20332-0001

No. Of Copies	Organization
6	Commander Naval Ordnance Station ATTN: P. L. Stang J. Birkett L Torreyson T. C. Smith D. Brooks Tech Library Indian Head, MD 20640-5000
1	AFSC/SDOA Andrews AFB, MD 20334
6	AFRPL (DYSC) ATTN: D. George J. N. Levine B. Goshgarian D. Thrasher N. Vander Hyde Tech Library Edwards AFB, CA 93523-5000
1	AFFDL ATTN: TST-Lib Wright-Patterson AFB, OH 45433
1	AFFTC ATTN: SSD-Tech LIb Edwards AFB, CA 93523
1	AFATL/DLYV Eglin AFB, FL 32542-5000
1	AFATL/DLXP Eglin AFB, FL 32542-5000
1	AFATL/DLJE Eglin AFB, FL 32542-5000
1	AFATL/DLODL ATTN: Tech Lib Eglin AFB, FL 32542-5000
1	AFWL/SUL Kirtland AFB, NM 87117

DISTRIBUTION LIST

No. Of Copies	Organization
1	NASA/Lyndon B. Johnson Space Center ATTN: NHS-22, Library Sectin Houston, TX 77054
1	AFELM, The Rand Corporation ATTN: Library D 1700 Main Street Santa Monica CA 90406-3297
1	General Applied Sciences Lab ATTN: J. Erdos Merrick & Stewart Avenues Westbury Long Isld, NY 11590
1	AAI Corporation ATTN: J. Herbert J. Frankle P. O. Box 6767 Baltimore, MD 21204
1	Aerodyne Research, Inc. Bedford Research Park ATTN: V. Yousefian Bedford, MA 01730
1	Aerojet Ordnance Company ATTN: D. Thatcher 2521 Michelle Drive Tustin, CA 92680
1	Aerojet Solid Propulsion Co. ATTN: P. Micheli Sacramento, CA 95813
1	Atlantic Research Corporation ATTN: M. K. King 5390 Cheorokee Avenue Alexandria, VA 22312-2302
1	AVCO Everett Rsch Lab ATTN: D. Stickler 2385 Revere Beach Parkway Everett, MA 02149-5936

No. Of Copies	Organization
1	Calspan Corporation ATTN: C. Morphy P. O. Box 400 Buffalo, NY 14225-0400
1	Foster Miller Associates ATTN: A. Erickson 135 Second Avenue Waltham, MA 02154
1	General Electric Company Armament Systems Dept. ATTN: M. J. Bulman, Room 1311 128 Lakeside Avenue Burlington, VT 05401-4985
1	IITRI ATTN: M. J. Klein 10 W. 35th Street Chicago, IL 60616-3799
1	Hercules Inc. Allegheny Ballistics Laboratory ATTN: R. B. Miller P. O. Box 210 Cumberland, MD 21501-0210
1	Hercules, Inc. Bacchus Works ATTN: K. P. McCarty P. O. Box 98 Magna, UT 84044-0098
1	Hercules, Inc. Radford Army Ammunition Plant ATTN: J. Pierce Radford, VA 24141-0299
1	Honeywell, Inc. Defense Systems Division ATTN: C. Hargreaves 5901 So. City Road 18 Edina, MN 55436

DISTRIBUTION LIST

No. Of Copies	Organization
1	Lawrence Livermore National Laboratory ATTN: L-355, A. Buckingham M. Finger P. O. Box 808 Livermore, CA 94550-0622
1	Lawrence Livermore National Laboratory ATTN: L-324 M. Constantino P. O. Box 808 Livermore, CA 94550-0622
1	Olin Corporation Badger Army Ammunition Plant ATTN: R. J. Thiede Baraboo, WI 53913
1	Olin Corporation Smokeless Powder Operations ATTN: Mr. McDonald P.O. Box 222 St. Marks, FL 32355-0222
1	Paul Gough Associates, Inc. ATTN: P. S. Gough P. O. Box 1614, 1048 South St. Portsmouth, NH 03801-1614
1	Physics International Company ATTN: Library H. Wayne Wampler 2700 Merced Street San Leandro, CA 94577-5602
1	Princeton Combustion Research Lab., Inc. ATTN: M. Summerfield 475 US Highway One Monmouth Junction, NJ 08852-9650

No. Of Copies	Organization
2	Rockwell International Rocketdyne Division ATTN: BA08 J. E. Flanagan J. Gray 6633 Canoga Avenue Canoga Park, CA 91304
1	Science Applications, Inc. ATTN: R. B. Edelman 23146 Cumorah Crest Drive Woodland Hills, CA 91364-3710
3	Thiokol Corporation Huntsville Division ATTN: D. Flanigan R. Glick Tech Library Huntsville, AL 35807
1	Scientific Research Assoc., Inc. ATTN: H. McDonald P.O. Box 498 Glastonbury, CT 06033-0498
1	Thiokol Corporation Wasatch Division ATTN: J. A. Peterson P. O. Box 524 Brigham City, UT 84302-0524
2	Thiokol Corporation Elkton Division ATTN: R. Biddle Tech Lib. P. O. Box 241 Elkton, MD 21921-0241
2	United Technologies Chemical Systems Division ATTN: R. Brown Tech Library P. O. Box 358 Sunnyvale, CA 94086-9998

DISTRIBUTION LIST

No. Of Copies	Organization
1	Veritay Technology, Inc. ATTN: E. Fisher 4845 Millersport Hwy. P. O. Box 305 East Amherst, NY 14051-0305
1	Universal Propulsion Company ATTN: H. J. McSpadden Black Canyon Stage 1 Box 1140 Phoenix, AZ 85029
1	Battelle Memorial Institute ATTN: Tech Library 505 King Avenue Columbus, OH 43201-2693
1	Brigham Young University Dept. of Chemical Engineering ATTN: M. Beckstead Provo, UT 84601
1	California Institute of Tech 204 Karman Lab Main Stop 301-46 ATTN: F. E. C. Culick 1201 E. California Street Pasadena, CA 91109
1	California Institute of Tech Jet Propulsion Laboratory ATTN: L. D. Strand 4800 Oak Grove Drive Pasadena, CA 91109-8099
1	University of Illinois Dept of Mech/Indust Engr ATTN: H. Krier 144 MEB; 1206 N. Green St. Urbana, IL 61801-2978
1	University of Massachusetts Dept. of Mechanical Engineering ATTN: K. Jakus Amherst, MA 01002

No. Of Copies	Organization
1	University of Minnesota Dept. of Mechanical Engineering ATTN: E. Fletcher Minneapolis, MN 55455
1	Case Western Reserve University Division of Aerospace Sciences ATTN: J. Tien Cleveland, OH 44135
3	Georgia Institute of Tech School of Aerospace Eng. ATTN: B. T. Zinn E. Price W. C. Strahle Atlanta, GA 30332
1	Institute of Gas Technology ATTN: D. Gidaspow 3424 S. State Street Chicago, IL 60616-3896
1	Johns Hopkins University Applied Physics Laboratory Chemical Propulsion Information Agency ATTN: T. Christian Johns Hopkins Road Laurel, MD 20707-0690
1	Massachusetts Institute of Technology Dept of Mechanical Engineering ATTN: T. Toong 77 Massachetts Avenue Cambridge, MA 02139-4307
1	G. M. Faeth Pennsylvania State University Applied Research Laboratory University Park, PA 16802

DISTRIBUTION LIST

No. Of Copies	Organization
1	Pennsylvania State University Dept. Of Mechanical Engineering ATTN: K. Kuo University Park, PA 16802
1	Purdue University School of Mechanical Engineering ATTN: J. R. Osborn TSPC Chaffee Hall West Lafayette, IN 47906
1	SRI International Propulsion Sciences Division ATTN: Tech Library 333 Ravenswood Avenue Menlo Park, CA 94025-3493
1	Rensselaer Polytechnic Inst. Department of Mathematics Troy, NY 12181
2	Director Los Alamos Scientific Lab ATTN: T3, D. Butler M. Division, B. Craig P. O. Box 1663 Los Alamos, NM 87544
1	Stevens Institute of Technology Davidson Laboratory ATTN: R. McAlevy, III Castle Point Station Hoboken, NJ 07030
1	Rutgers University Dept. of Mechanical and Aerospace Engineering ATTN: S. Temkin University Heights Campus New Brunswick, NJ 08903
1	University of Southern California Mechanical Engineering Dept. ATTN: OHE200, M. Gerstein Los Angeles, CA 90007

No. Of Copies	Organization
2	University of Utah Dept. of Chemical Engineering ATTN: A. Baer G. Flandro Salt Lake City, UT 84112
1	Washington State University Dept. of Mechanical Engineering ATTN: C. T. Crowe Pullman, WA 99163

Aberdeen Proving Ground

Dir, USAMSAA
ATTN: AMXSY-D
AMXSY-MP, H. Cohen
Cdr, USATECOM
ATTN: AMSTE-TO-F
AMSTE-CM-F, L. Nealley
Cdr, CSTA
ATTN: STECS-AS-H, R. Hendricksen
Cdr, CRDC, AMCCOM
ATTN: SMCCR-RSP-A
SMCCR-MU
SMCCR-SPS-IL

10	Central Intelligence Agency Office of Central Reference Dissemination Branch Room GE-47 HQS Washington, D.C. 20502

☆U.S. GOVERNMENT PRINTING OFFICE: 491-390/20016

USER EVALUATION SHEET/CHANGE OF ADDRESS

This Laboratory undertakes a continuing effort to improve the quality of the reports it publishes. Your comments/answers to the items/questions below will aid us in our efforts.

1. BRL Report Number __________ Date of Report __________

2. Date Report Received __________

3. Does this report satisfy a need? (Comment on purpose, related project, or other area of interest for which the report will be used.) __________

4. How specifically, is the report being used? (Information source, design data, procedure, source of ideas, etc.) __________

5. Has the information in this report led to any quantitative savings as far as man-hours or dollars saved, operating costs avoided or efficiencies achieved, etc? If so, please elaborate. __________

6. General Comments. What do you think should be changed to improve future reports? (Indicate changes to organization, technical content, format, etc.)

CURRENT ADDRESS

Name

Organization

Address

City, State, Zip

7. If indicating a Change of Address or Address Correction, please provide the New or Correct Address in Block 6 above and the Old or Incorrect address below.

OLD ADDRESS

Name

Organization

Address

City, State, Zip

(Remove this sheet along the perforation, fold as indicated, staple or tape closed, and mail.)

FOLD HERE

Director
U.S. Army Ballistic Research Laboratory
ATTN: SLCBR-DD-T
Aberdeen Proving Ground, MD 21005-5066

NO POSTAGE
NECESSARY
IF MAILED
IN THE
UNITED STATES

OFFICIAL BUSINESS
PENALTY FOR PRIVATE USE, $300

BUSINESS REPLY MAIL
FIRST CLASS PERMIT NO 12062 WASHINGTON, DC

POSTAGE WILL BE PAID BY DEPARTMENT OF THE ARMY

Director
U.S. Army Ballistic Research Laboratory
ATTN: SLCBR-DD-T
Aberdeen Proving Ground, MD 21005-9989

FOLD HERE

END

DTIC

5-86